OPTICAL KLYSTRON ENHANCEMENT TO SASE X-RAY FELS

Yuantao Ding*, Paul Emma, Zhirong Huang†, SLAC,Menlo Park, CA 94025, USA
Vinit Kumar‡, ANL, Argonne, IL 60439, USA.

Abstract

The optical klystron enhancement to self-amplified spontaneous emission (SASE) free electron lasers (FELs) is studied in theory and in simulations. In contrast to a seeded FEL, the optical klystron gain in a SASE FEL is not sensitive to any phase mismatch between the radiation and the microbunched electron beam. The FEL performance with the addition of four optical klystrons located at the undulator long breaks in the Linac Coherent Light Source (LCLS) shows significant improvement if the uncorrelated energy spread at the undulator entrance can be controlled to a very small level. In addition, FEL saturation at shorter x-ray wavelengths (around 1.0 Å) within the LCLS undulator length becomes possible. We also discuss the application of the optical klystron in a compact x-ray FEL design that employs relatively low electron beam energy together with a shorter-period undulator.

INTRODUCTION

An x-ray free electron laser (FEL) operated in the self-amplified spontaneous emission (SASE) mode is the primary candidate for the next-generation light source and is under active development around the world [1, 2, 3]. In such a device, based on the achievable electron beam qualities such as peak current and transverse emittances, the total length of the undulator required to reach the x-ray intensity saturation usually exceeds 100 m. The electron beam energy spread is typically too small to affect the SASE performance.

To enhance the FEL gain, the optical klystron concept has been invented by Vinokurov and Skrinsky [4] and has been successfully implemented in many FEL oscillator facilities such as the Duke FEL [5]. An optical klystron consists of two undulators, separated by a dispersive section (a magnetic chicane). The dispersive section converts beam energy modulation into density modulation and hence speeds up the gain process. Theoretical studies of the optical klystron in high gain FEL amplifiers show that its performance depends critically on the electron beam energy spread [6, 7, 8]. More recently, Neil and Freund [9] have studied a distributed optical klystron configuration using the LCLS parameters. Based on the FEL amplifier simulations that start with a coherent seed, they point out that the performance of the optical klystron for short-wavelength FELs is very sensitive to the exact slippage of

* Electronic address: ding@slac.stanford.edu. On leave from IHIP, Peking University, Beijing, China.
† Electronic address: zrh@slac.stanford.edu.
‡ Current address: G-20, ADL Building, Raja Ramanna Centre for Advanced Technology, Indore-452013, INDIA.

the electron beam relative to the radiation in the dispersive section. Thus, the magnetic fields of the chicane must be carefully designed and controlled to very high precision.

Motivated by the very small uncorrelated energy spread of the electron beam that has been measured in a photo-cathode RF gun [10], we study the possible optical klystron enhancement to SASE x-ray FELs. We show that a SASE optical klystron is not sensitive to the relative phase of the electron beam to the radiation as long as the electron slippage length in the dispersive section is much longer than the coherence length of the radiation. Based on extensive SASE simulations, we illustrate the gain enhancement of the optical klystron to the LCLS and a compact x-ray FEL scheme.

ONE-DIMENSIONAL ANALYSIS

In this section, we analyze an optical klystron configuration with a magnetic chicane between two high-gain FEL undulators and extend the previous theoretical treatments [6, 7, 8] to the high-gain SASE operating mode. A detailed description may be found in [11].

A magnetic chicane introduces an energy-dependent longitudinal delay of the electron relative to the radiation, which can be expressed as a change of the radiation phase "seen" by the electron:

$$\Delta\theta = -\frac{k_r R_{56}}{2} + k_r R_{56}\delta \qquad (1)$$

Here $\lambda_r = 2\pi/k_r = 2\pi c/\omega_r$ is the FEL resonant wavelength, R_{56} is the momentum compaction of the chicane, and $\delta = (\gamma - \gamma_0)/\gamma_0$ is the relative energy deviation. The first term in Eq. (1) describes the overall phase slippage between the FEL radiation and the reference electron having the energy $\gamma_0 mc^2$, and the second term describes the relative phase change for an electron with a slightly different energy. Following the one-dimensional (1D) theory of Kim [8] but keep the overall phase slippage, we write down the optical klystron (OK) enhancement factor to the radiation field E_ν at the scaled frequency $\nu = \omega/\omega_r$:

$$R(\nu) \equiv \frac{E_\nu^{\text{OK}}}{E_\nu^{\text{no OK}}}$$

$$= \frac{1 - \int d\xi \frac{dV(\xi)/(d\xi)}{(\mu-\xi)^2} e^{-i\rho k_r \nu R_{56}\xi} e^{ik_r \nu R_{56}/2}}{1 + 2\int d\xi \frac{V(\xi)}{(\mu-\xi)^3}} \qquad (2)$$

where $\xi = \delta/\rho$ is the normalized energy variable, ρ is the FEL Pierce parameter [12], μ is the complex growth rate of the radiation field in each undulator, $\mu = (-1 + i\sqrt{3})/2$ for a beam with a vanishing energy spread, and $V(\xi)$ is the

energy distribution of the electron beam with the normalization $\int V(\xi)d\xi = 1$.

The first term in the numerator of Eq.(2) represents the contribution from the radiation in the first undulator, while the second term in the numerator represents the contribution of the microbunched electron beam. For a seeded FEL with $\nu = 1$, $k_r R_{56}/2 = 2\pi n(n = 1, 2, 3, \ldots)$ yields a nearly matched phase (i.e., constructive interference between two terms). The optical klystron is then optimized for a matched phase. However, in the hard x-ray wavelength range, changing R_{56} of the chicane by a fraction of 1 Angstrom can result in a complete phase mismatch. Thus, there can be large fluctuations in the radiation power due to small fluctuations in the magnetic fields as observed in Ref. [9]. Even when the magnetic fields are held constant, a small energy jitter (on the order of 10^{-4}) can also mismatch the phase.

Nevertheless, SASE FELs start from shot noise and have a relatively wide bandwidth. For a given value of R_{56}, the phase may be mismatched for one particular wavelength but may be properly matched for another wavelength within the SASE bandwidth. Thus, we should integrate over the SASE spectrum $S(\nu)$ to obtain the optical klystron power gain factor as:

$$G = \int d\nu |R(\nu)|^2 S(\nu) \qquad (3)$$

For an electron beam with a Gaussian energy distribution of rms width $\sigma_\delta \ll \rho$ (i.e., $\sigma_\xi \ll 1$), we can integrate Eq. (1) over energy and Eq. (3) over frequency (assuming a Gaussian average SASE spectrum) to obtain

$$G = \frac{1}{9}\left[5 + D^2 \exp(-D^2\sigma_\xi{}^2) + 2\sqrt{3}D\exp\left(-\frac{D^2\sigma_\xi{}^2}{2}\right)\right.$$
$$+ \left(4 + \sqrt{3}D\exp\left(\frac{-D^2\sigma_\xi{}^2}{2}\right)\cos\left(\frac{D}{2\rho}\right)\right.$$
$$\left.- D\exp\left(\frac{-D^2\sigma_\xi{}^2}{2}\right)\sin\left(\frac{D}{2\rho}\right)\right)\exp\left(\frac{-D^2\sigma_\nu{}^2}{8\rho^2}\right)\bigg] \qquad (4)$$

where $D = k_r R_{56}\rho$. The power gain factor G as a function of the chicane strength R_{56} is shown in Fig. 1 for two typical values of the rms energy spread σ_δ, assuming a typical rms SASE bandwidth $\sigma_\nu = \rho$.

When R_{56} is very small, the optical klystron operates as a phase shifter, and the FEL power is oscillatory depending on the relative phase between the radiation and the electron beam. As $k_r R_{56}\sigma_\delta \rightarrow 1$, the optical klystron gain peaks and starts to decay exponentially due to the smearing effect of the intrinsic energy spread. Thus, the phase matching is no longer important when the optical klystron is near its peak performance.

A simple physical picture emerges in the time domain. The path length difference between the SASE radiation and the electron beam passing the dispersive section is about $R_{56}/2 \approx 1/(2k_r\sigma_\delta) = \lambda_r/(4\pi\sigma_\delta)$ at the optimal chicane
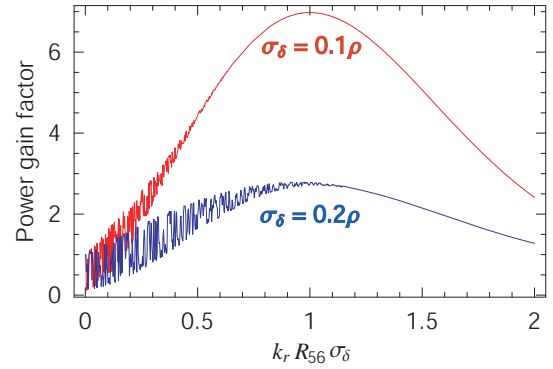

Figure 1: (color) 1D power gain factor with relative energy spread $\sigma_\delta = 0.1\rho$ (red line) and $\sigma_\delta = 0.2\rho$ (blue line)

setting. Since the typical SASE coherence length is on the order of $\lambda_r/(4\pi\rho)$ [13, 14], it is much smaller than the path length difference introduced by the chicane when the beam energy spread $\sigma_\delta \ll \rho$ (a necessary condition for the operation of the high-gain optical klystron). Therefore, there is no place for the electron beam to match the radiation phase after the beam is slipped from the SASE radiation more than a few temporal spikes. The radiation power averaged over many statistically independent spikes is then not sensitive to the exact slippage introduced by the chicane.

UNCORRELATED ENERGY SPREAD

Since the uncorrelated energy spread plays a crucial role for the gain enhancement of the optical klystron, we analyze here two main sources of energy spread. One is from the gun and the linac, which forms the initial energy spread at the entrance of the FEL undulator; while the other is the quantum diffusion due to spontaneous radiation along the undulator, which leads to an increase of energy spread after the electron beam is injected into the undulator. The uncorrelated energy spread of electron beams generated from a photocathode rf gun can be extremely small, at an rms value of 3 to 4 keV from both measurements [10] and simulations. Nevertheless, a microbunching instability driven by longitudinal space charge and coherent synchrotron radiation in the accelerator system may be large enough to significantly degrade the beam qualities including the energy spread [15, 16]. This microbunching instability occurs at much longer wavelengths than the FEL microbunching and requires much larger R56 (from bunch compressor chicanes) than the optical klystron chicanes. To maintain a relatively small energy spread after compression and acceleration, a laser heater [15, 16] will be used in the LCLS injector to increase the rms energy spread from 3 to 40 keV. After a total compression factor of about 30, the slice rms energy spread at the undulator entrance can be controlled to 1×10^{-4} at 14 GeV, which is tolerable for the SASE FEL at 1.5 Å. However, considering the gain enhancement of the optical klystron (see Fig.1), a smaller energy spread (e.g., 5×10^{-5} or 0.1ρ) is desirable. This may be achiev-

able by dropping the heater-induced energy spread to 20 keV at the expense of the increased microbunching instability gain. For a smooth enough photocathode drive laser profile, this higher instability gain may still be tolerable after acceleration and bunch compression. Thus, the final slice energy spread at the undulator entrance may be kept at 5×10^{-5} for the LCLS.

The energy diffusion due to spontaneous radiation along the undulator was discussed by Saldin et al [17]. This energy diffusion rate increases with γ^4 and K^3 for $K^2 \gg 1$. For the LCLS at $\lambda_r = 1.5$ Å and $K = 3.5$, the rms energy spread increases from initial value of 5×10^{-5} to 1×10^{-4} at the undulator position of 40 m due to the spontaneous radiation. We will include this effect in the FEL simulations to be discussed below.

THREE DIMENSIONAL SIMULATIONS

Three-dimensional (3D) simulation code Genesis 1.3 [18] is used to explore the LCLS gain enhancement with a distributed optical klystron configuration for two different radiation wavelengths of 1.5 Å and 1.0 Å and a very compact x-ray FEL at 1.5 Å.

We place four 4-dipole chicanes in the first four long breaks between LCLS undulator sections (at 12, 24, 36, and 48 m) to form a distributed optical klystron configuration. For each chicane, the optimal gain enhancement is obtained by scanning the chicane dipole magnetic field strength. Two initial rms energy spread values of 1×10^{-5} and 5×10^{-5} at the entrance of the undulator are used in the 3D simulations. While we consider the energy spread of 5×10^{-5} may be achievable in the LCLS with a reasonably smooth drive-laser profile or with the low-charge option [19], the energy spread of 1×10^{-5} requires to switch off the laser heater completely and is probably not allowed by the microbunching instability in the linac. It is still included in the simulations in order to study the best possible optical klystron performance and the influence of spontaneous energy diffusion in the undulator.

Fig. 2 shows the FEL power gain along the undulator with and without optical klystrons at the resonant wavelength of 1.5 Å for $K = 3.5$ (the current LCLS design parameters), with an electron peak current of 3.4kA and normalized rms emittance of 1.2 μm. The saturation length is shortened by 13 m using these optical klystrons with an initial energy spread of 5×10^{-5} and R_{56} of the chicanes at around 0.25μ m (with a small variation for each chicane). Note that a 10% variation of the chicane R_{56} values does not make a visible difference for the FEL output power.

To allow for the LCLS to reach 1.0 Å without increasing the beam energy, the undulator gap may be increased by 2 mm to reduce the undulator parameter to $K = 2.7$. The 3D simulation results are presented in Fig. 3, using a peak current of 3.4kA and normalized rms emittance of 1.2 μm. Without any optical klystron, the nominal LCLS beam cannot reach SASE saturation at this wavelength. With the addition of four optical klystrons as described here, the sat-
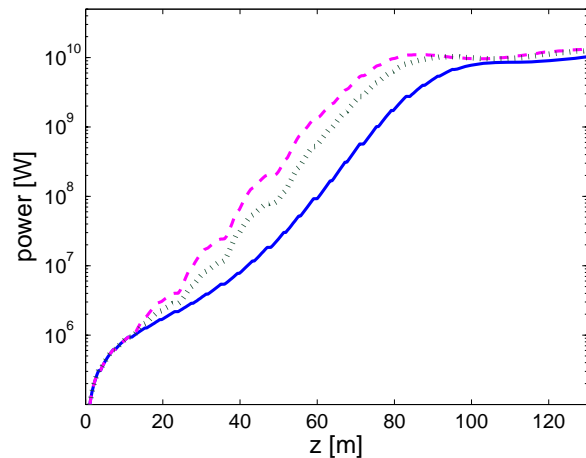

Figure 2: (color) SASE FEL power along the undulator without any optical klystron (blue solid curve), and with 4 optical klystrons for the initial rms energy spread of 1×10^{-5} (magenta dashed curve) and 5×10^{-5} (green dotted curve). The FEL wavelength is 1.5 Å, and the undulator parameter $K = 3.5$.
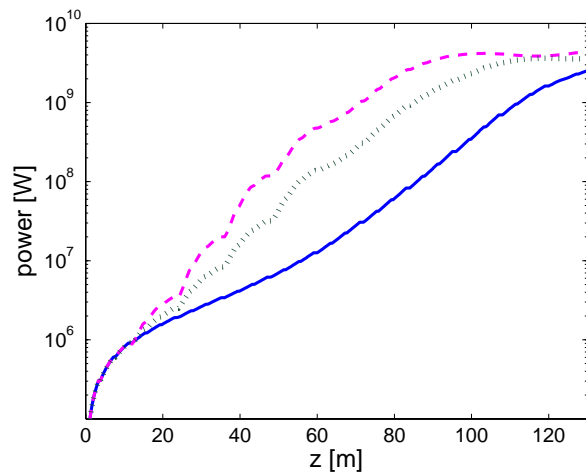

Figure 3: (color) SASE FEL power along the undulator without any optical klystron (blue solid curve), and with 4 optical klystrons for the rms energy spread of 1×10^{-5} (magenta dashed curve) and 5×10^{-5} (green dotted curve). The FEL wavelength is 1.0Å, and the undulator parameter $K = 2.7$.

uration distance is shortened by about 26 m and is well within the LCLS total undulator length. At this K value and using a lower beam energy (11.0 GeV), simulations also show the FEL at 1.5 Å approximately save 25 m of saturation length compared to that without any optical klystron.

It is clear from these numerical examples that a simultaneous reduction in beam energy and undulator parameter for the same radiation wavelength is beneficial for the optical klystron enhancement, where the energy diffusion due
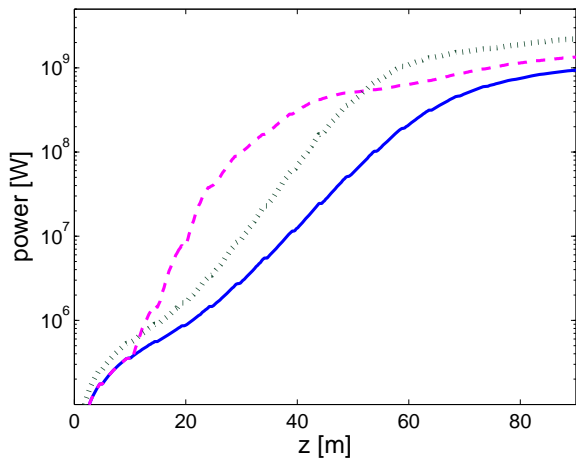
Figure 4: (color) SASE FEL power along the undulator at a peak current of 2kA without any optical klystron (blue solid curve) and with 4 optical klystrons (magenta dashed curve), and at peak current of 3kA without any optical klystron (green dotted curve). The FEL wavelength is 1.5 Å and the undulator parameter $K = 1.3$.

to spontaneous radiation in the undulator is much reduced. Inspired by the Spring-8 Compact SASE Source (SCSS) design [3], we study the possibility of using a relatively low energy electron beam together with a short-period undulator to drive a compact x-ray FEL with the aid of the distributed optical klystrons. A 1.5-cm period in-vacuum undulator with $K = 1.3$ is used according to the design parameters in SCSS. To produce 1.5-Å FEL radiation, the necessary electron energy is about 5 GeV. Rather than a standard peak current of 3 kA as described in Ref. [3], we assume a lower peak current of 2 kA and an rms energy spread of 100 keV (or 2×10^{-5}) at the undulator entrance. A smaller peak current allows for a smaller energy spread and may also help reduce the microbunching instability gain in the accelerator, as well as any wakefield effect in the small gap, in-vacuum undulator. Fig. 4 shows the simulation results for the SASE mode without any optical klystron (for both 3-kA and 2-kA bunches) and with four optical klystrons (for a 2-kA bunch). The latter saturates at around 50 m of the undulator distance, which is still about 10 m shorter than the higher-current case without any optical klystron.

SUMMARY

The small, experimentally measured uncorrelated energy spread from RF guns offers the opportunity to consider applications of optical klystrons in x-ray FELs. In contrast to a seeded FEL, our study shows that the optical klystron gain is not sensitive to the relative phase between the SASE radiation and the electron beam, and that the radiation power is very stable with a relatively large tuning range of optical klystrons. 3D simulations of the LCLS with a distributed optical klystron configuration show significant gain enhancement if the slice energy spread at the undulator entrance can be controlled to a very small level. The improved performance can be used to obtain the FEL saturation at shorter x-ray wavelengths for a fixed undulator length or to relax the stringent requirement on the beam emittance. The exploration of optical klystrons in a very compact x-ray FEL also indicates promising results. Therefore, we think that the optical klystron configuration can be an easy "add-on" to SASE x-ray FELs provided that electron beams with very small energy spreads are obtainable at the final beam energy.

REFERENCES

[1] Linac Coherent Light Source (LCLS) Conceptual Design Report, SLAC Report No. SLAC-R-593, 2002.

[2] Technical Design Report, DESY TESLA-FEL Report, 2002.

[3] SCSS X-FEL conceptual design report, RIKEN, 2002.

[4] N.A. Vinokurov and A.N. Skrinsky, Preprint of INP 77-59, Novosibirsk, (1977).

[5] Y. K. Wu *et al.*, Phys. Rev. Lett. 96, 224801 (2006).

[6] R. Bonifacio, R. Corsini, and P. Pierini, Phys. Rev. A 45, 4091 (1992).

[7] N.A. Vinokurov, Nucl. Instrum. Methods Phys. Res. A 375, 264 (1996).

[8] K.J. Kim, Nucl. Instrum. Methods Phys. Res. A 407, 126 (1998).

[9] G.R. Neil and H.P. Freund, Nucl. Instrum. Methods Phys. Res. Sec. A 475, 381 (2001).

[10] M. Huning and H. Schlarb, in Proceedings of the 2003 Particle Accelerator Conference, Portland, 2074 (2003).

[11] Y. Ding, P. Emma, Z. Huang, V. Kummar, Phys. Rev ST Accel. Beams 9, 070702 (2006).

[12] R. Bonifacio, C. Pellegrini, and L.M. Narducci, Opt. Commun. 50, 373 (1984).

[13] R. Bonifacio, L. De Salvo, P. Pierini, N. Piovella, and C. Pellegrini, Phys. Rev. Lett. 73, 70 (1994).

[14] E.L. Saldin, E.A. Schneidmiller, and M.V. Yurkov, Opt. Commun. 148, 383 (1998).

[15] E. Saldin, E. Schneidmiller, and M. Yurkov, TESLA-FEL-2003-02, DESY (2003).

[16] Z. Huang *et al.*, Phys. Rev. ST Accel. Beams 7, 074401 (2004).

[17] E.L. Saldin, E.A. Schneidmiller, and M.V. Yurkov, Nucl. Instrum. Methods Phys. Res. A 381, 545 (1996).

[18] S. Reiche, Nucl. Instrum. Methods Phys. Res. A 429, 243 (1999).

[19] P. Emma *et al.*, the Proceedings of 2005 Particle Accelerator Conference, Tennessee, 344, (2005).